The Student-Organized Local Atmospheric Research (SOLAR) Experiment: Microclimatic Properties and Their Impact on Environmental Growing Conditions

Abstract

Agrivoltaics is a potential answer to growing renewable energy demands. It involves growing crops inside solar fields. The impact of solar panels on their surrounding microclimate is not well understood. Previous research has been done in arid areas, where shade from solar panels has a pronounced effect on soil moisture. Our study was done at O'Brien and Moray solar fields in south-central Wisconsin. We measured the microclimatic conditions at these fields by deploying weather station tripods, soil moisture sensors, tethersondes, kestrel drops, and a gas scouter at both sites. Measurements were taken at different sites: (1) under the solar panel (2) between two rows of panels and (3) in an open field adjacent to the solar field (control). Our study takes place from 2024 March 9 to 2024 April 5. Our results demonstrate that the position of solar panels creates a wind tunnel effect and blocks wind from certain directions. Also, the rate of soil moisture depletion is lower inside the solar field than outside. Methane concentrations are lower under the solar panels, while CO_2 levels remain constant between panels. The tethersonde reveals a temperature inversion about two meters above the ground, which is the approximate height of the solar panels. Temperature and relative humidity are not preferentially cooler or warmer under the solar panels. Lastly, the average dew point at the wetter Moray field is higher than at O'Brien. Our results provide evidence that solar panels can affect the microclimate. These effects should be further investigated to determine the viability of crops under these microclimatic conditions.

Introduction

As debates surrounding climate change mitigation take place in various sectors of the world, another topic that comes up is how to shift our energy consumption away from fossil fuels and towards renewable energy all while keeping up with energy and resource demands. One promising solution is the use of agrivoltaics to address the growing challenges surrounding sustainable agriculture, energy demand, and water resources. The practice of agrivoltaics encompasses the integration of photovoltaic infrastructure onto an agricultural field, which reduces land use competition amongst solar panel farms and crop land all while supplying both clean energy and food. However, this integration has been met with concerns over how solar panel arrays affect growing conditions of crops and microclimates of agricultural lands; though much research is yet to be completed regarding these concerns.

Expand on environmental growing conditions and why we chose our variables
Agrivolatics maximizes land usage by allowing crops to grow underneath and between solar panel arrays. Solar arrays provide more shade in comparison to crops grown in open fields and growing conditions such as temperature and others have the potential of being affected. In addition, wind tunnels are also created through the panels. In order to obtain well rounded data on the microclimate of agricultural fields that are being affected by agrivolatics, the environmental conditions we focused on were temperature underneath solar panels, soil moisture, CO2 concentration, and shortwave radiation. Atmospheric profiles were also observed.

Our research is a continuation of previous years of agrivoltaic experimentation focusing on meteorological measurements. The 2018 SAVANT project honed in on nighttime atmospheric profiles,

moisture drainage and aerosol transportation. CHEESEHEAD focuses on the use of flux towers to measure atmospheric spatial variability in the forest. Our spring 2024 projects couples SAVANT and CHEESEHEAD as well as previous 404 experiments to further the observations of microclimatic conditions in Solar Farm Arrays. The hope is that our research will continue the conversations and studies in the field of agrivotaics to potentially see impacts of solar panel farms on vegetation.

Hypothesis and Scientific Objectives

The goal of this experiment was to validate the following statements:

1. Near-surface atmospheric conditions like temperature, wind speed, and wind direction are modified due to placement and angle of PV panels.
2. Vegetation under solar panels will see an increase in CO2 and decrease in CH4 as opposed to concentrations outside of panels.
3. Solar panels create shade, reducing sunlight on the soil and thereby lowering evaporation, which helps retain moisture, unlike the control sites.
4. Upward and downward longwave radiative fluxes will be larger at the control sites compared to the sites with solar panels.

Methods for Data Acquisition

Site Description

The AOS 404: Meteorological Measurements course worked alongside professionals at Madison Gas & Electric to access photovoltaic (PV) systems at two sites in the Madison area: the Moray Solar Field and the O'Brien Solar Field. Each of these sites contained multiple solar arrays with natural vegetation growing underneath the panels. Data was collected over a four week period with weekly maintenance/data collection sessions.

Tripods

A total of five tripods were deployed at the two experimental sites; three at the O'Brien site and two at the Moray site. At O'Brien, one tripod was installed in the West array (A), one in the East array (C), and one adjacent to the East array (B) to be used as the control. At Moray, one tripod was installed inside the PV array (E) and one adjacent to the PV array (D) to be used as the control.

Each of the tripods were intended to be installed in an identical fashion. Tripods were matched with their respective data loggers (A-E) and measurement tools. Each of the five HOBO tripods included a cup anemometer and wind vane directed to true North, placed on a cross bar 3m above the ground. Below the cross bar, a small solar panel is attached to the pole facing south to best capture sunlight for logger charging. Underneath the solar panel, a temperature/humidity sensor is attached to the pole facing true North, and a barometric pressure sensor is connected below. A soil moisture sensor was placed six inches (15 cm) into the ground next to the base of tripods to measure the volumetric water content indirectly in soil. Each of these instruments is then connected to a HOBO U30 Weather Station Data Logger.

Data was retrieved from the data loggers at a sampling interval of one minute with a recording interval of five minutes. Data retrieved included incoming shortwave radiation, wind direction, wind speed, gust speed, air temperature, dew point temperature, relative humidity, and soil moisture.

Picarro Gas Scouter

The Picarro Gascouter G4301 backpack is a portable battery powered gas concentration analyzer used for high precision greenhouse gas measurements, specifically carbon dioxide (CO2) and methane (CH4). These high precision measurements continuously measured CO2 and CH4 and soil flux measurements. Measurements were taken at both sites, and at every tripod station A-E, with two of those sites as control sites. Data was taken on two days - March 15th and April 5th, 2024. However, only April 15th provided data that could be analyzed, and is therefore the day elaborated on in this paper. The main goal of using the Picarro Gascouter was to compare measurements taken at tripod sites between solar panels and at vegetation underneath solar panels, comparing the flux of both gasses.

Differences in CO2 and CH4 were measured in parts per million(ppm). Measurements were taken at each tripod and a nearby solar panel, with the instrument running for approximately 5 minutes at each location. The process of taking measurements and time increments can be found in the tables below. For control tripods, data was only collected at said tripod considering there were no nearby solar panels. Additionally, soil and plant conditions varied over the different locations, so qualitative data was also collected to aid in analysis. Qualitative data measurements may also be found in the tables below. In between intervals of soil data collection, the Picarro was pointed upwards, towards fresh air, in order to make results for the soil flux more apparent in data analysis.

Kestrels

Two Kestrel drop devices were deployed underneath the solar panels, to measure how conditions there varied relative to away from the panels: one at Moray and one at O'Brien, each centrally located within the field. On 15 March 2024, a week after they were first deployed, they were both moved slightly to correct discrepancies noted due to contact between the Kestrel drops and adjacent metal structures, observed when comparing current observations from our devices to a handheld device. These devices recorded temperature and dew point data, which were compared to information collected by the National Weather Service at Truax Field (the official weather station for Madison) and from the nearby tripods.

Our drops were each associated with one team member's cellphone, where data were stored in a designated application and then uploaded to our shared drive for analysis. They collected data every five minutes, which we then took hourly averages of to reduce the effects of random short-lived spikes in numbers and make the data set easier for us to handle during analysis.

Tethersonde

A tethersonde was deployed at the east array of O'Brien in order to better understand how the air is being modified as it passes over and through the solar panels. For this project, we were primarily concerned with the lowest levels of the atmosphere. Since a traditional windsonde would pass through this layer quickly, it was decided to attach the windsonde to a kite string, also called a tethersonde. This records the temperature, humidity, pressure, altitude, GPS location, heading, and more variables that were not used in this experiment. The one negative effect of attaching the windsonde to a string is the elimination of wind speed and direction measurements. During a traditional windsonde, wind speed and direction are calculated based on GPS location. Since we were not allowing the windsonde to travel freely with the flow, wind speed, and direction cannot be calculated.

When arriving at the field for the day, the direction of the wind is noted. The start of each pass of the tethersonde would begin upwind and then travel in the direction of the wind into the solar panel array.

By using the WS-250 for Windows program and a radio receiver, we were able to verify the tethersonde was recording data in real time. Prior to going into the field, we marked every 2.5 m on the kite string to measure variables at discrete intervals. This procedure was only valid for days with somewhat calm conditions. At higher heights, even the smallest gust of wind had the capability of tangling the tethersonde in the solar panels. This effect was minimized by using a larger amount of helium in the balloon so the buoyancy associated with it counteracted the gusts of wind. The tethersonde was moved across the field at a near constant rate for all levels. This process would be repeated until the highest level, allowed by the wind, was recorded.

In order to achieve findings from the data, there were some computations needed with the data. First, in order to isolate paths in the right direction, data was filtered by heading. This allowed us to only use the data during the path that followed the wind. Additionally, an interpolation of the latitude and longitude was needed to get a continuous path. These changes to the data allowed us to make conclusions about how the air was being modified over the field.

Results

Tripods

(a) Experimental Shortwave Radiation Deviations from Control

We hypothesized that incoming shortwave radiation would be less within the PV array than at control sites due to the shade that the solar panels would induce throughout the day. In order to determine the validity of this, we took hourly resamples of the shortwave radiation data collected from each of the three O'brien site tripods, computed the deviations of experimental data from control data, and plotted a time series encompassing the whole duration of the experiment (Fig. 1a). For ease of interpretation, the first day of data is plotted separately (Fig. 1b) in order to better visualize the pattern unveiled through this method.

Overarchingly, we find in Figure 1a that there is a diurnal cycle in experimental deviations in shortwave radiation from control, with experimental sites (i.e. sites within the PV arrays) demonstrating the expected negative anomaly for part of every day and an unexpected *positive* anomaly for another part of the day. Looking at Figure 1b., experimental deviations are negative in the early morning (peaking on the order of ~100 W/m^2) to approximate solar noon and positive – though less-so than they are negative in the early half of the day – throughout the afternoon until sunset (peaking on the order of ~50 W/m^2). It is not entirely clear what causes this diurnal cycle, particularly with positive experimental deviations; we believe there may be an additional component of shortwave reflectance from the solar panels themselves for the latter half of the day that could potentially increase the total incoming shortwave radiation measured by the tripod pyranometer.

(b) Directionally-Filtered Wind Speed

On the basis of known surface roughness impacts on wind speed, we hypothesized that wind speed would overall be slower at experimental sites than at control sites. Later, while in the field, this hypothesis was revised to include a directional dependence statement: wind speed would be slower at experimental sites when wind is oriented *orthogonal* to the PV arrays and faster when wind is oriented *parallel* to the PV arrays. To test this, we filtered week 1 wind speeds at each O'brien site by direction within +/- 5º of true north, east, south, and west and generated scatter plots with data from each of the three sites for westerly (Fig. 2a), easterly (Fig. 2b), northerly (Fig. 2c), and southerly (Fig. 2d) winds.

In general, there does appear to be a directional dependence for wind speed within PV arrays; however, it is a more complex relationship than whether the winds are oriented orthogonal or parallel to the arrays. Figure 2a shows that, while there are plenty of control data points for westerly winds, there are very few experimental data points, and they do not necessarily reveal a statistically significant correlation between westerly orientation and slower wind speed. A more reasonable statement is that westerlies are typically blocked by solar panels altogether or directionally modified by surface roughness throughout the array.

Figure 2b demonstrates an even more complex relationship; we observe that easterly winds at experimental sites are highly turbulent, and the east experimental site features overall faster easterly wind speeds than both the west and control sites. This could be due to the simple fact that the east site receives easterly winds before either of the other sites would and thus would likely experience less modification of easterlies than the other two sites. Additionally, there could be a potential trapping of easterly winds between the solar panel rows by a slight micro-temperature-inversion at solar panel height unveiled by the tethersonde, which could promote the formation of turbulent eddies and cause a wide distribution of easterly wind speed readings at experimental sites.

Figure 2c shows that northerly-oriented winds are fairly variable, but all northerly wind speeds greater than 6 knots are experimental readings; this means there could be an observable wind-tunnel effect within PV arrays when winds are oriented northerly-parallel to the panel rows. Finally, Figure ?d shows that southerly winds were observed exclusively at the experimental sites with a bias toward faster wind speeds. This demonstrates the same wind-tunnel effect revealed by Figure ?c, but there also appears – based upon the lack of southerly data observed at the control site – to be a directional modification by the solar panel rows that would guide southwesterly or southeasterly flow into a southerly orientation within the PV arrays.

(c) Pressure-Wind Speed Deviation Correlation

One pattern revealed by additional analysis of O'brien experimental wind speed deviations from control was an apparent barometric pressure dependence (Fig. 3). Generally, the trend we observe is that, any time there is a relative low spike in pressure, experimental wind speed deviations become more negative, meaning that wind speeds at the O'brien experimental sites are slower than control wind speeds. Any time there is a relative high spike in pressure, experimental wind speed deviations become closer to zero.

It is not readily obvious why this occurs. However, it is plausible that, because low pressure is often more associated with higher wind variability and faster wind speeds, there could be more significant modification of wind speed by the PV arrays such that turbulent mixing results in negative experimental deviations. Conversely, high pressure is more associated with calmer winds, thus causing less turbulent wind speed modification as flow traverses across PV arrays and resulting in near-zero experimental deviations.

Soil Moisture Observations

Four soil moisture sensors were installed on tripods, with each pair set up in different fields in Morey and O'Brien. Within each pair, one sensor was placed at the control site and the other among the solar arrays. The sensors were installed six inches (15 cm) into the ground next to the base of tripods.

Observations from the sensors indicate a notable difference in soil moisture levels between the control sites and the sites among the solar arrays. Soil moisture depletion at the control site is greater than at the sites among the solar arrays, suggesting that the latter maintain higher soil moisture levels (Figure 4). Spikes observed in the data from both the control sites and the solar sites suggest that the sensors are synchronized, providing some validation for the results.

There is a strong, positive correlation between soil moisture and relative humidity at both sites, but the nature of this relationship differs between tripods placed outside (control sites) and inside (experimental sites) the solar field ($CC > 0.45$; $p < 0.001$). At O'Brien, soil moisture varies more with relative humidity for the tripods placed within the solar field (Figures 5,6). The control site at O'Brien has fairly constant soil moisture values until relative humidity exceeds 90%, at which point the soil moisture values rise exponentially (Figure 6). These patterns may be explained by rainfall patterns within the solar field. The control site may be more sensitive to rainfall because it is exposed to the elements. The experimental site is in an alleyway, so rainfall may be blocked by the solar panels, limiting the maximum amount of rainfall observed here. In the context of this correlation, high relative humidity values ($RH > 90\%$) at the control site are likely indicative of large rainfall events that can easily increase soil moisture. However, high relative humidity values at the experimental site do not necessarily yield higher soil moisture values due to their localized microclimates.

A few hypotheses can be drawn from these findings. (1) Solar panels create shade, reducing the amount of direct sunlight hitting the soil, which in turn can lower evaporation rates and help retain moisture. (2) Solar panels can act as windbreaks, decreasing wind speed in the areas between the arrays. This reduction in wind can lead to reduced evaporation, contributing to higher soil moisture levels. (3) Shaded areas, like those between solar panels, tend to be cooler. The cooler temperatures can further reduce evaporation rates and potentially mitigate soil heat stress, leading to higher moisture retention. (4) Solar panels might also act as rain collectors, directing rainwater to certain areas and thus increasing moisture concentration in those regions. (5) The installation of solar panels might impact the soil structure and compaction, which could alter its water retention capacity.

Kestrels

Surface temperatures measured under the solar panels by the Kestrel drops are not preferentially warmer or colder than surface temperatures from the nearby control tripods (Figure 8). Temperatures are higher under the solar panels only about 50% of the time at both sites, demonstrating an even split between warmer and cooler periods throughout this study (Figures 7, 8). After the daily low is reached, from 12:00-18:00 UTC, temperatures are lower under the solar panels than at the control tripods. Incoming solar radiation may be blocked by the solar panels in the morning because the sun is not at a high enough angle to shine under them (Figure 7). About an hour before the daily high is reached, it becomes hotter under the solar panels than at the control tripods. At 18:00 UTC, the temperature under the solar panel reaches a higher daily maximum (Figure 7). The kestrel drop retains that extra heat until the next morning at 12:00 UTC when it once again becomes colder than the control tripods (Figure 7). In the afternoon, solar panels may produce more heat energy and absorb more solar radiation. This may explain why it is warmer under the solar panel, even during the late evening hours.

Relative humidity is not preferentially higher or lower under the solar panels (Figure 9). The relative humidity profile demonstrates the diurnal cycle, with lower values in the morning and higher values in the afternoon (Figure 9). It is noted that peaks and depressions in relative humidity at observed at the same time the difference in temperature between kestrel and tripod changes signs (Figure 10)

We used data from the National Weather Service as a control for comparing the data from our Kestrel drops. Over this period, the average temperature at Truax Field was 37.8° F, ranging from a high of 66.2° F on March 12 at 21:00 to a low of 18.8° F on March 23 at 12:00 (Figure 11a). The average dew point was 25.9° F, ranging from a high of 48.2° F during much of the day on March 25 to a low of 0.2° F on March 20 at 22:00 (Figure 11b). NWS data are rounded to the nearest degree Celsius, so many smaller and more-temporary changes in temperature and dew point are missed, but this still represents general trends well.

Picarro Gas Scouter

When measuring the soil flux on the ground near Tripod A (Figure 14), methane began to lower gradually, and then dropped about 4 minutes into the measurement. When the Picarro was oriented towards clean air, methane concentrations stayed low and stagnant until the Picarro was moved to measure under the solar panel. The methane initially spikes and decreases again after 3-4 minutes. Contrary to this, CO2 measurements under the tripod are relatively unchanged to the clean air measurements, but does have a drop in CO2 about the same time that corresponding methane concentrations drop. Under the solar panel, CO2 concentrations increase exponentially, negatively correlating with the methane concentrations for under the panel.

Tripod C (Figure 15) had almost identical methane and CO2 results for soil flux underneath the tripod, where levels of methane stay pretty constant until a few minutes into measurement when values begin to drop. CO2 stays constant throughout the entire measurement period. The corresponding solar panel follows the general trend for methane, aside from the values themselves being much lower. The CO2 for this also behaves interestingly, where there is a sharp increase after a minute of measurement, and then a very sharp decrease in CO2 concentrations. Considering this takes place in the middle of measurements, and there is very little airflow into the chamber, this may be an error in the data recording itself.

The two control groups for O'Brien and Morrey, Tripods B (Figure 16) and D (Figure 17) respectively, follow similar trends to those seen in the solar fields, where methane concentrations initially stay relatively consistent, and then towards the end of the time interval, drop. Similarly to the tripods located in between solar panels, CO2 concentrations stay relatively low and constant throughout the measurement period.

Tripod E (Figure 18) is particularly interesting, because it doesn't seem to follow the same patterns as seen at the other tripods. With this one, methane concentrations are much larger under the solar panels compared to the tripods, and CO2 sees a much larger increase in concentration underneath the tripod compared to the solar panel. Additionally, the overall shape of the curve is much different than what we see for methane measurements, where it appears the methane is constantly decreasing over the measurement period. One possible explanation for this could be due to the type of vegetation at each site, considering the most clear results came from Tripods A and E, which both had lush vegetation being recorded, but have different mixes. This therefore suggests that the vegetation at sites of Morey and O'Brien may have different methane and CO2 outputs based on the type of plants.

Overall methane follows similar patterns for both near the tripod and under the solar panel, yet overall methane concentrations are lower underneath the solar panel. However, CO2 tends to be more consistent (though concentrations vary) by the tripods, and much more CO2 under the panels. When considering the qualitative data taken at each tripod site, there does seem to be a relationship between how lush the vegetation is and CO2 concentrations. In the instance in Tripod A where we had a large strip

of thicker grass, CO2 concentrations rose exponentially compared to the other sites, even if those other sites had some form of vegetation. This could be due to the timing of the year, and that in general, there isn't a lot of vegetation around to soak up CO2. Therefore, the processes being picked up by the Picarro sensor are most likely on the microbial level. This means that small organisms potentially living in the grass are emitting more CO2 than what the grass itself can take in, therefore causing a net increase in concentrations at the ground.

Tethersonde

Due to inclement weather, the tethersonde was only deployed on 2 days. The first deployment was on 15 March from 18:52-19:46 UTC. Data for this run was collected at several height levels, along a full east-west transect in the eastern O'Brien field. The direction of the mean wind on this day was westerly, so data was filtered to only use westerly headings from 45^{o} to 135^{o}. The second deployment was on 5 April from 19:11-19:31 UTC. Data for this run was collected across 3 different height levels at 2.5 m, 5 m, and 7.5 m, with a partial north-south transect completed at each height. From the second deployment, highly variable tethersonde heights associated with small wind gusts were noted. The measured altitude during the 7.5 m run had an average height above ground level (AGL) of 4 m, with deviations as high as 6 m and as low as 2 meters (Figure 12). Due to this fluctuation, the analysis was primarily conducted via vertical profiles of temperature. The data from the first deployment was divided into 3 regions. The "West", "Central", and "East" regions were designated by all data points within a longitude range of (-89.4552^{o},-89.4541^{o}), (-89.4540^{o},-89.4528^{o}), and (-89.4527^{o},-89.4515^{o}) respectively. In each of these regions, low-level profiles of temperature were constructed via scatter plots (Figure 13). The vertical depth of these profiles extends from 983.4 to 982 hPa.

One result from this analysis of the 15 March data is that the "West" and "East" regions have well-mixed temperature profiles. The "East" region has a constant temperature profile with height, as would be expected over such a small vertical depth in a well-mixed environment. There is some variability in temperature, with a standard deviation of 0.373 ^{o}C throughout the profile. The "West" region has far more variability with a standard deviation of 0.857 ^{o}C throughout the profile. Despite this variability, there is a clear trend that the temperature profile remains constant in these regions. The "Central" region features a different trend. This region has a clear inversion near the surface. The average temperature within the surface layer (983.4-983.2 hPa) is 11.9 ^{o}C. This is topped by a layer (983.2-982.8 hPa) in which the average temperature is 12.6 ^{o}C. The temperature spread is not highly variable within these layers and appears to closely follow this inversion trend. We were unable to perform a similar analysis with the data from the 5 April deployment, as we did not perform a complete transect across the field.

This inversion is present in the "Central" region but is not an obvious feature in the "East" or "West" regions. The height of this inversion is on the order of 0.5 hPa (~2.5 meters) which is the height of the solar panels. It may be caused by reduced surface heating as the panels block much of the incoming radiation. It had also rained the day before on 14 March, and the wet soil characteristics may have had a latent cooling effect. The net result of these effects may have allowed this stable layer to persist so late into the afternoon in the center of the field. On the edges of the solar field, the inversion breaks earlier in the day and can mix with the outside conditions. This stable layer may reduce turbulent mixing beneath the solar panels and have impacts on plant growth. Future experiments can be set up to more efficiently analyze the low-level temperature profile at different times of the day to see the true prevalence of this stable boundary layer.

Data Discrepancies and Error

Tripods

At the Moray site, solar panels were incorrectly placed on tripods D and E upon installation meaning no viable data was collected during the first week of deployment. Additionally, at the Moray site there were issues with data logger relaunching, leading to tripod E missing its first two weeks of data. At the O'Brien field, the temperature/humidity sensor on tripod B was broken during the second week check-in. To remedy this, the temperature sensor from tripod A was moved to tripod B to have a full control dataset. Across all five of the tripods, there was a time divergence issue after the first week of data collection due to the data loggers being relaunched at different times. There was also an issue with unit disagreement as when each data logger was relaunched, the variable units were automatically reset to their default settings. Manual conversions were made across the datasets to ensure units were consistent throughout the course of the four weeks.

Kestrels

As mentioned, there was a change in siting between the first week of the experiment and the final three weeks. The data from the afternoon of 15 March onward are more accurate because the sensors were not making direct contact with the metal of the solar panels. It is also worth noting that the NWS data we compared the Kestrel data to was measured in degrees Celsius, while the Kestrel data were measured in tenths of a degree Fahrenheit. Therefore, differences of less than 1.8 F between NWS data and Kestrel data are not always significant.

Picarro Gas Scouter

Errors with the Picarro mostly stem from the instrument being in close proximity to humans emitting CO2, which was often picked up at the beginning or end of measurement intervals. Additionally, not every tripod or solar panel had the same vegetation or microbial makeup, which could impact raw values of the results.

The vacuum chamber that collected data was relatively air tight, but not completely. There could be error from moving air getting into the chamber and slightly altering results, and may be responsible for some of the odd behavior seen in some of the results.

During data recording and analysis, it was noticed the Piccaro is fifteen minutes ahead of the normal scheduled time. During analysis, human error may have occurred in interpretation of data during certain times of the day with this discrepancy in a time difference. Times were noted at the best estimated guess accounting for this difference.

Tethersonde

Similar to the gas scouter, some errors in the tethersonde data came from proximity to humans. On the 15 March deployment, the tethersonde continuously recorded data as we walked back and forth. On return trips, the tethersonde was held and the temperature sensor may have been impacted by its proximity to the hand. This anomalous data has mostly been eliminated from filtering by eastward headings, but some error points may still exist in the data. Additionally, there was one period on 15 March in which the tethersonde became caught on a solar panel. These data points were identified by a cluster of anomalously high temperatures and were removed from the dataset.

Conclusion

Leila

A scientific procedure this lengthy and detailed has potential for greater implications in the future. Our times of measurement were limited to our class time slot, so most of our observations were taken in the hours between 1- 4 PM CT. Taking these measurements at all times of day can tell us what we would expect given variations in solar fluxes. We were also limited by our seasons; it would be more interesting to conduct the same experiment throughout all times of year, especially the growing and harvest seasons. It would also be interesting to look at how vegetation composition impacts the amount of methane and CO2 emitted under the solar panels, and especially to take note of exactly which vegetation type was used at each site.

Overall, we have come to several conclusions in comparing our collected observations. Wind velocities are impacted by the presence of solar fields, as shown by the tripod data collection. From this, we can expect that the air is modified at a shallow depth above the panels as well. We have also found that temperature and relative humidity underneath the solar panels is not preferentially warmer or cooler than the control sites, which we did not expect given our hypothesis. However, soil moisture depletion is lower under the solar panels than at the control sites, allowing the soil to retain more moisture for longer periods of time. Based on the many findings of this experiment, the assumption that an agrivoltaic field has an impact on plant productivity underneath can be made.

Figures

Tripods

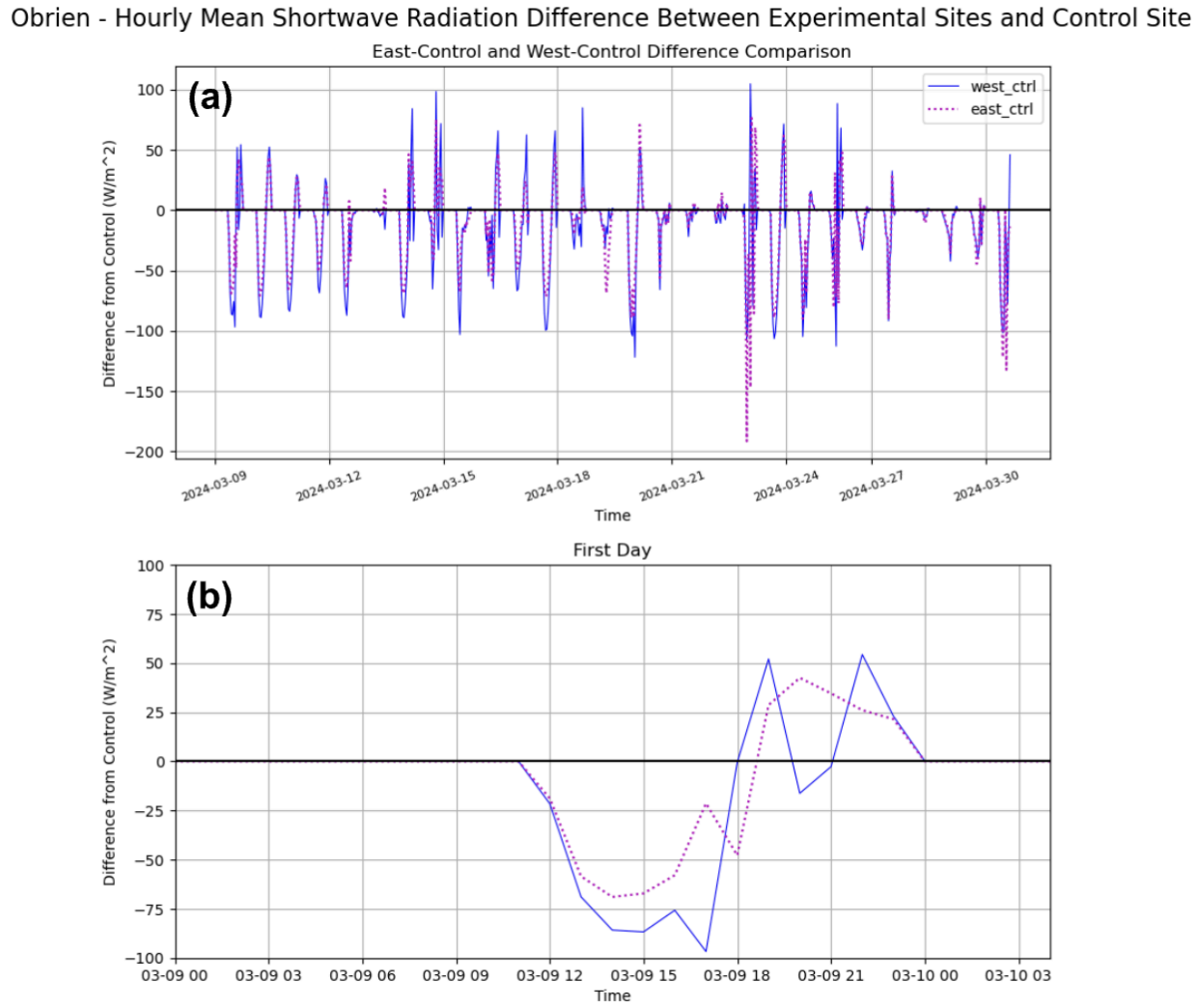

Figure 1. O'brien hourly-resampled experimental deviations of incoming shortwave radiation from control with (a) a full-duration time series, and (b) first-day sample for ease of visualization. The solid blue line characterizes the west experimental site's shortwave radiation deviations from control, and the dotted pink line characterizes the east experimental site's shortwave radiation deviations from control.

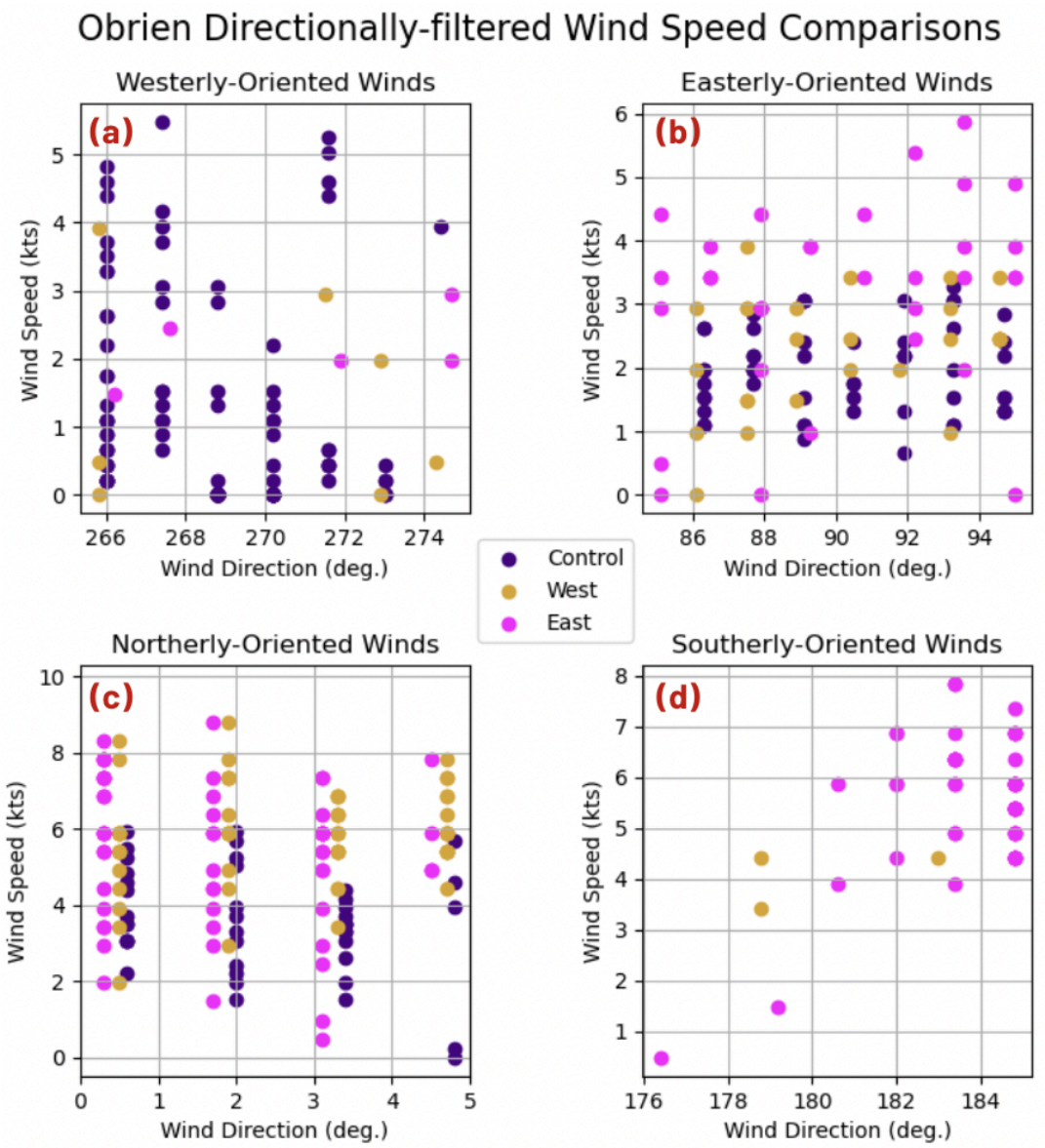

Figure 2. O'brien week 1 directionally-filtered wind speeds at each site for (a) westerly winds, (b) easterly winds, (c) northerly winds, and (d) southerly winds. Indigo points represent control wind speeds, yellow points represent west experimental site wind speeds, and pink points represent east experimental site wind speeds.

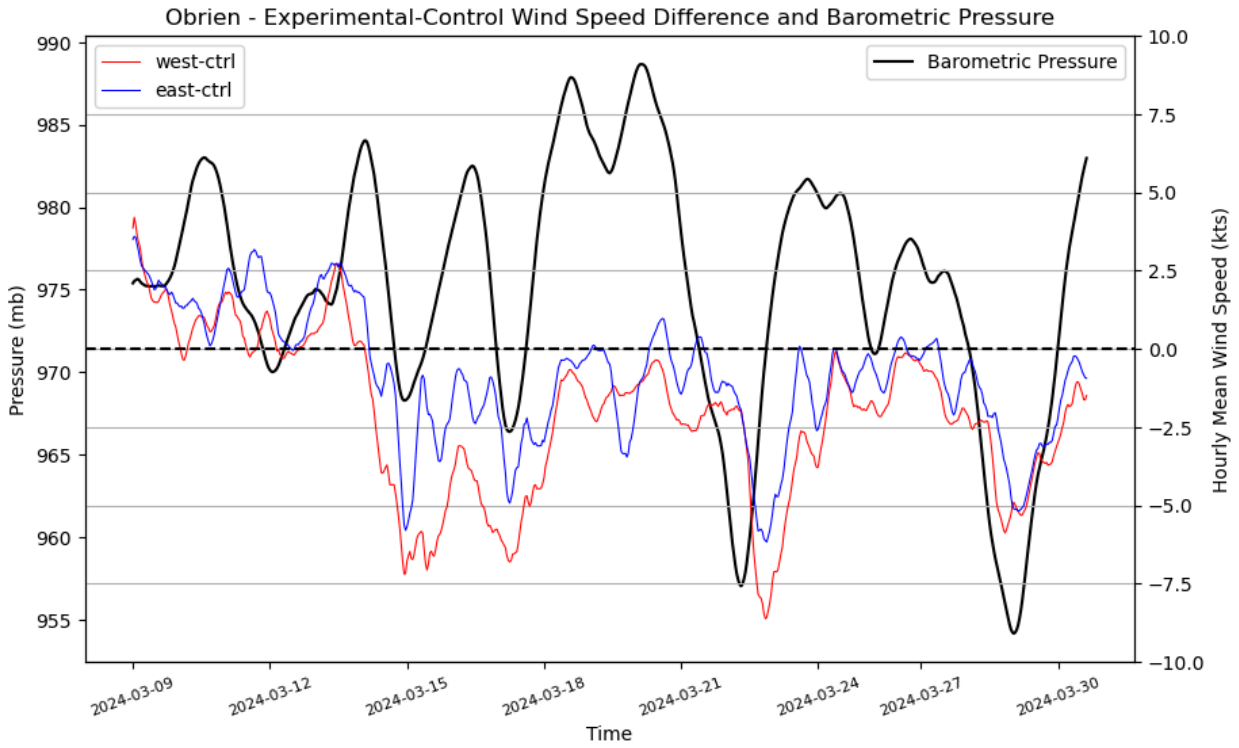

Figure 3. O'brien hourly mean barometric pressure (black), west experimental site wind speed deviation from control (red), and east experimental site wind speed deviation from control (blue).

Soil Moisture

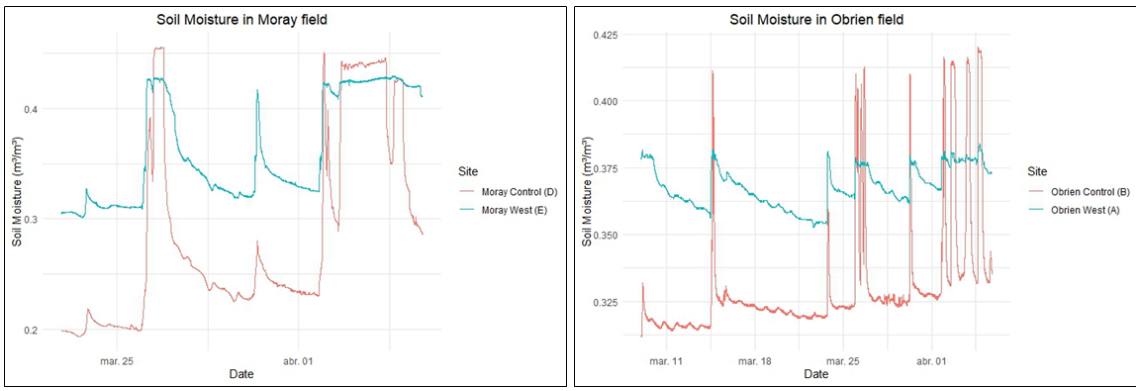

Figure 4. Soil moisture in m^3/m^3 at Moray and O'Brien. Turquoise lines are the control sites. Brown lines are the experimental sites within the solar field.

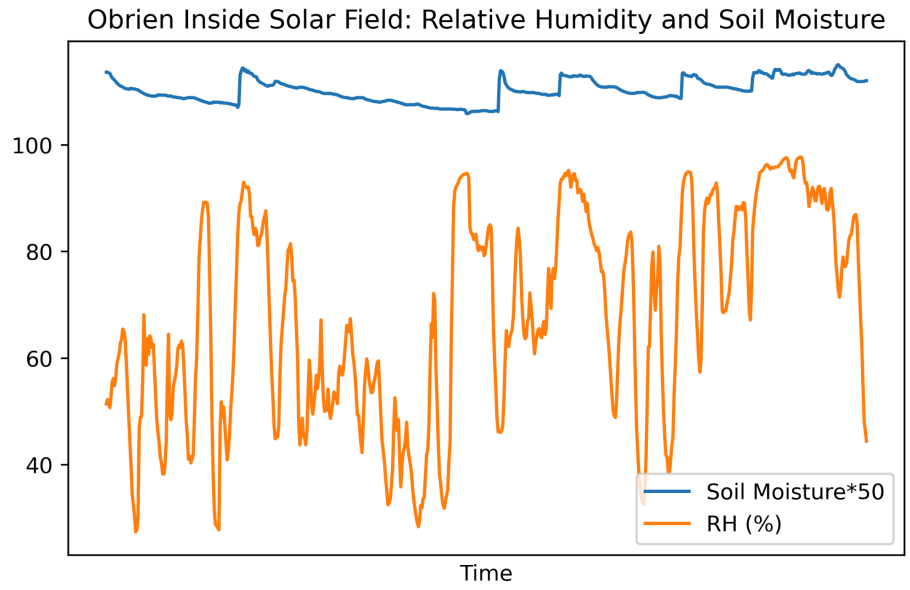

Figure 5. Soil moisture and relative humidity between 2024 9 March and 2024 5 April inside the O'Brien solar array. Soil moisture (blue line) in m^3/m^3 multiplied by a factor of 50. RH (orange line) in percent. Note how spikes in RH correspond to subsequent spikes in soil moisture values.

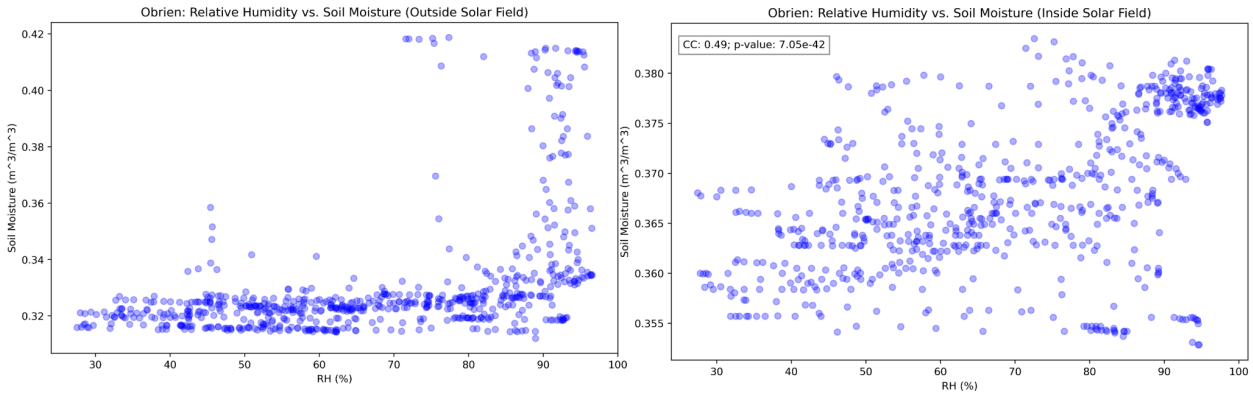

Figure 6. Relative humidity plotted against soil moisture at O'Brien outside (left plot) and inside (right plot) solar field.

Kestrels

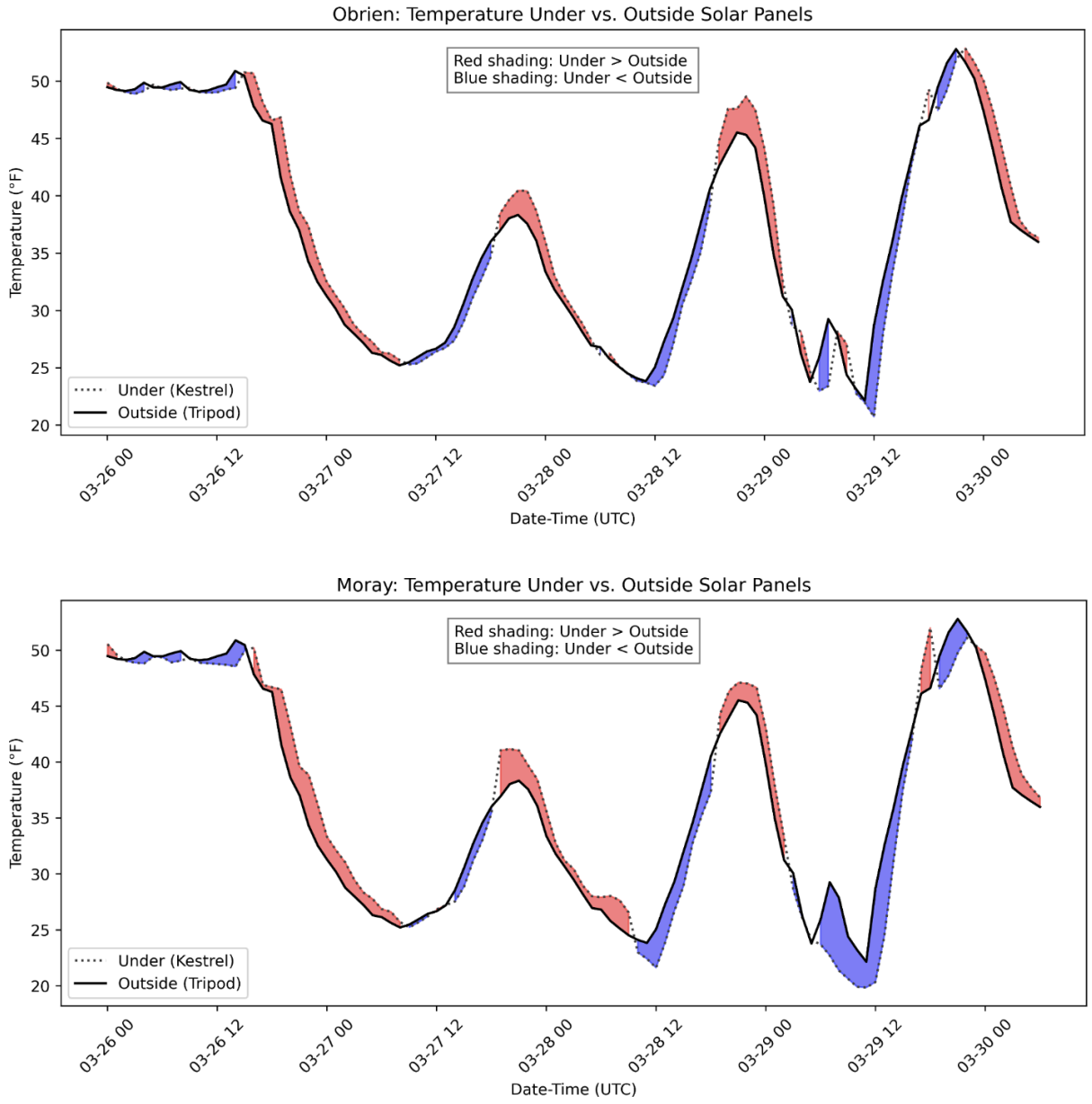

Figure 7. Surface temperatures in degrees Fahrenheit over 4 days (1) under the solar panel (kestrel drops) and (2) outside the solar field (control tripods). Timestamps are in UTC. Red shading represents periods when the temperature under the solar panels is warmer than at control sites (Blue is the opposite). The dotted line is the kestrel drop's temperature measurements. The solid line is the tripod's temperature measurements at the control sites.

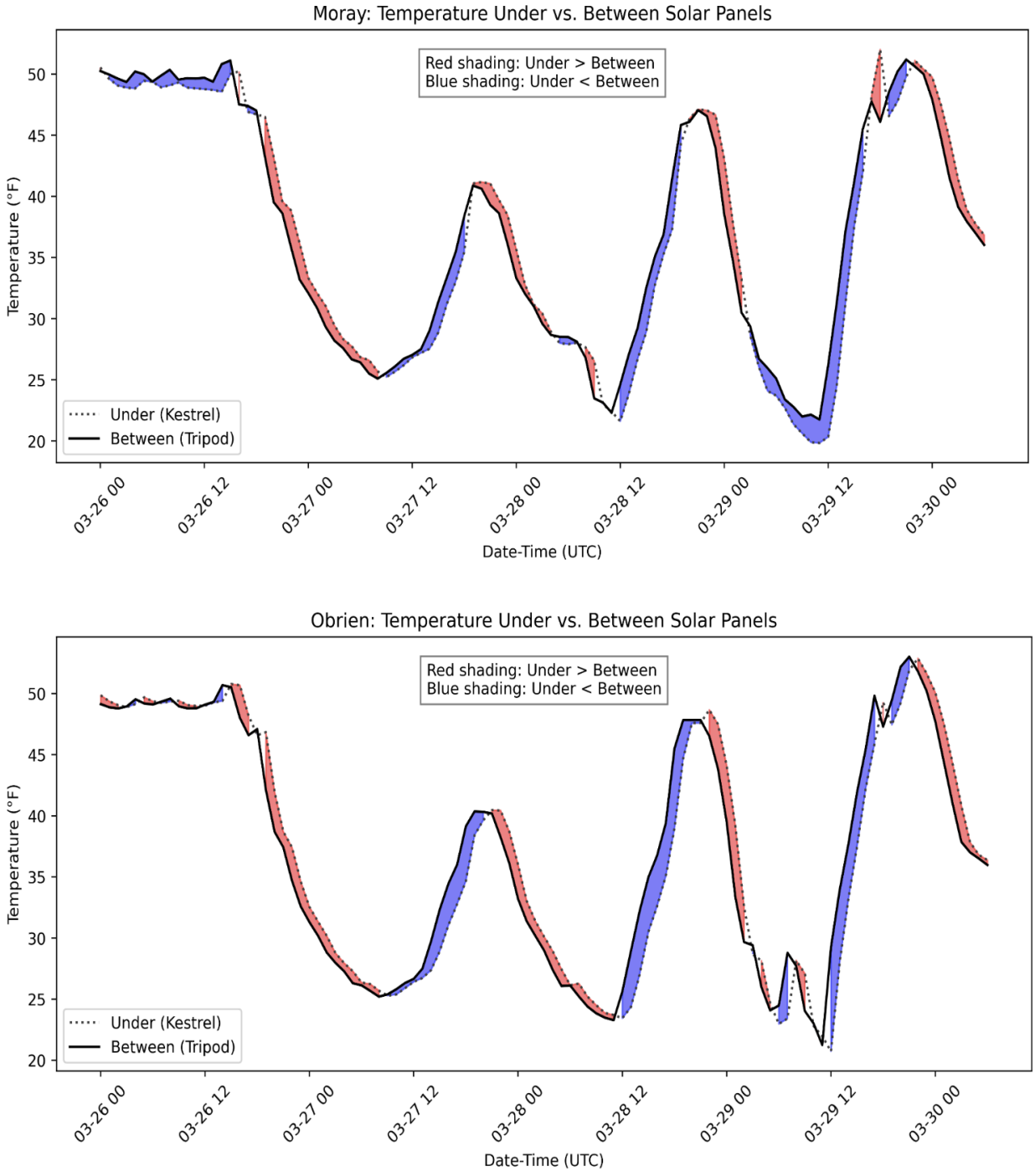

Figure 8. Surface temperatures in degrees Fahrenheit over 4 days (1) under the solar panel (kestrel drops) and (2) inside the solar field (control tripods). Timestamps are in UTC. Red shading represents periods when the temperature under the solar panels is warmer than at control sites (Blue is the opposite). The dotted line is the kestrel drop's temperature measurements. The solid line is the tripod's temperature measurements at the control sites.

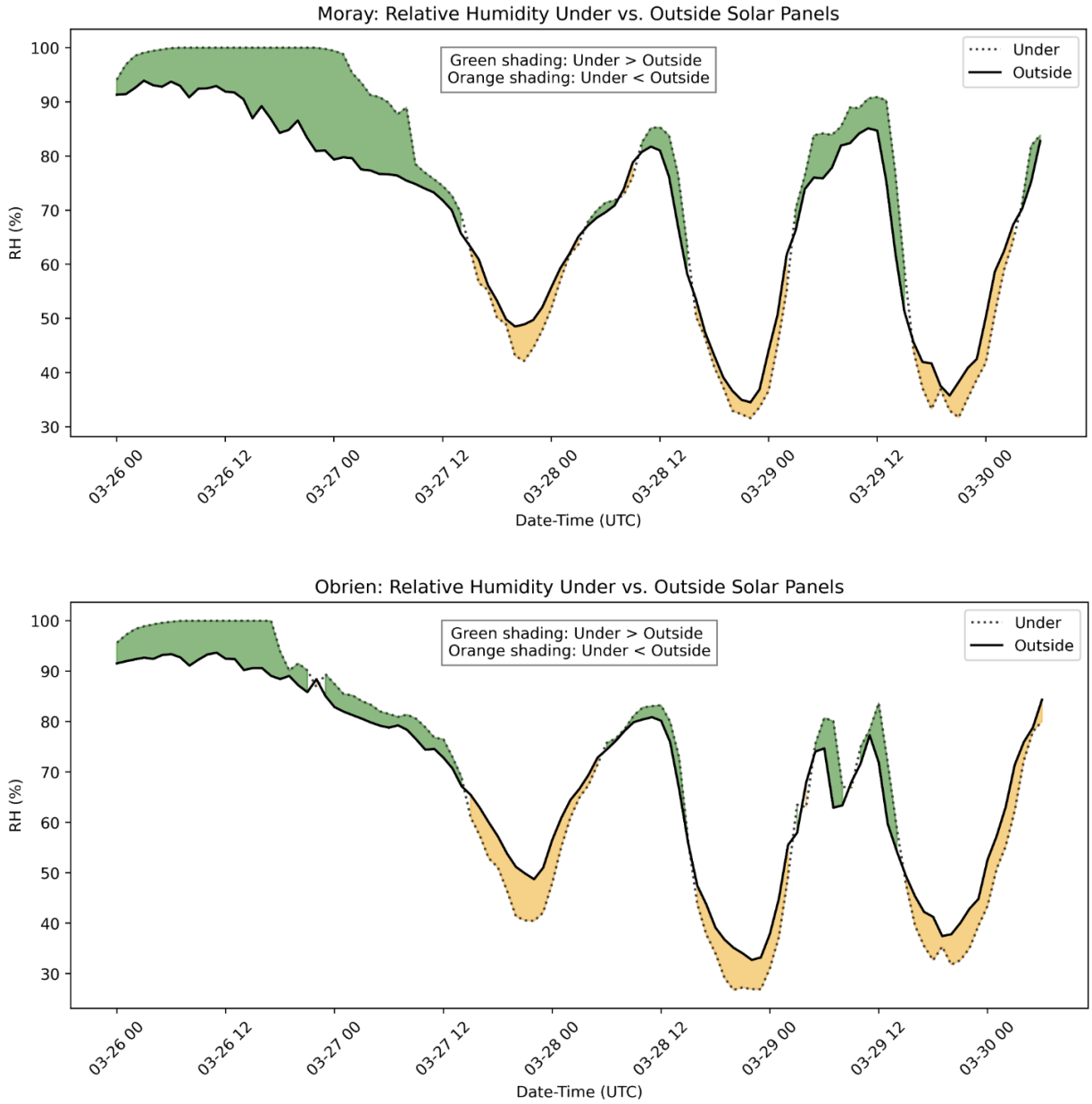

Figure 9. Relative Humidity (RH) percentage over 4 days (1) under the solar panel (kestrel drops) and (2) outside the solar field (control tripods). Timestamps are in UTC. Green shading represents periods when the RH under the solar panels is higher than at control sites (yellow is the opposite). The dotted line is the kestrel drop's RH measurements. The solid line is the tripod's RH measurements at the control sites.

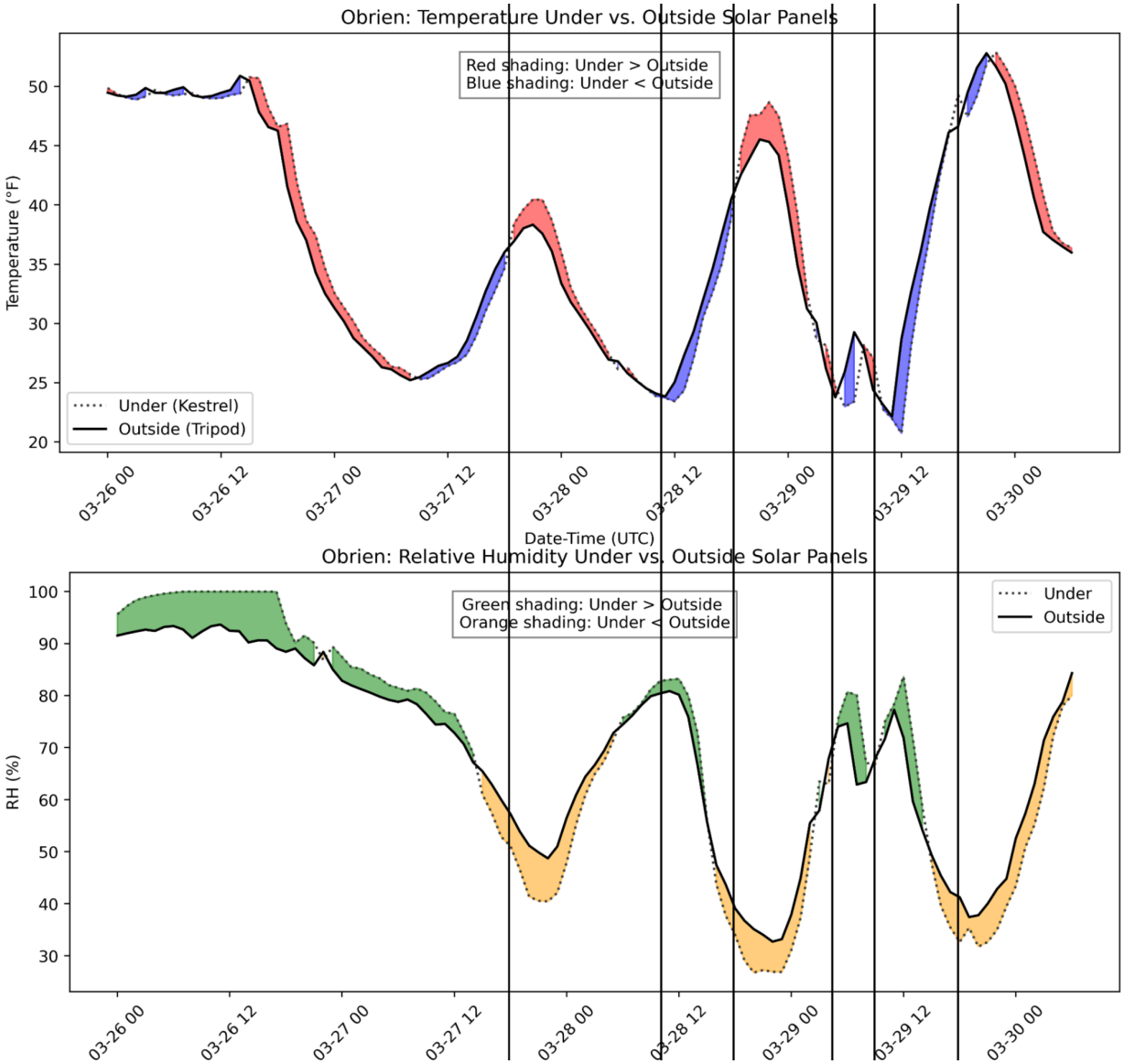

Figure 10. Relative humidity and surface temperatures over 4 days. Vertical black lines cross the same timestamp in each figure to demonstrate the connection between RH and surface temperature.

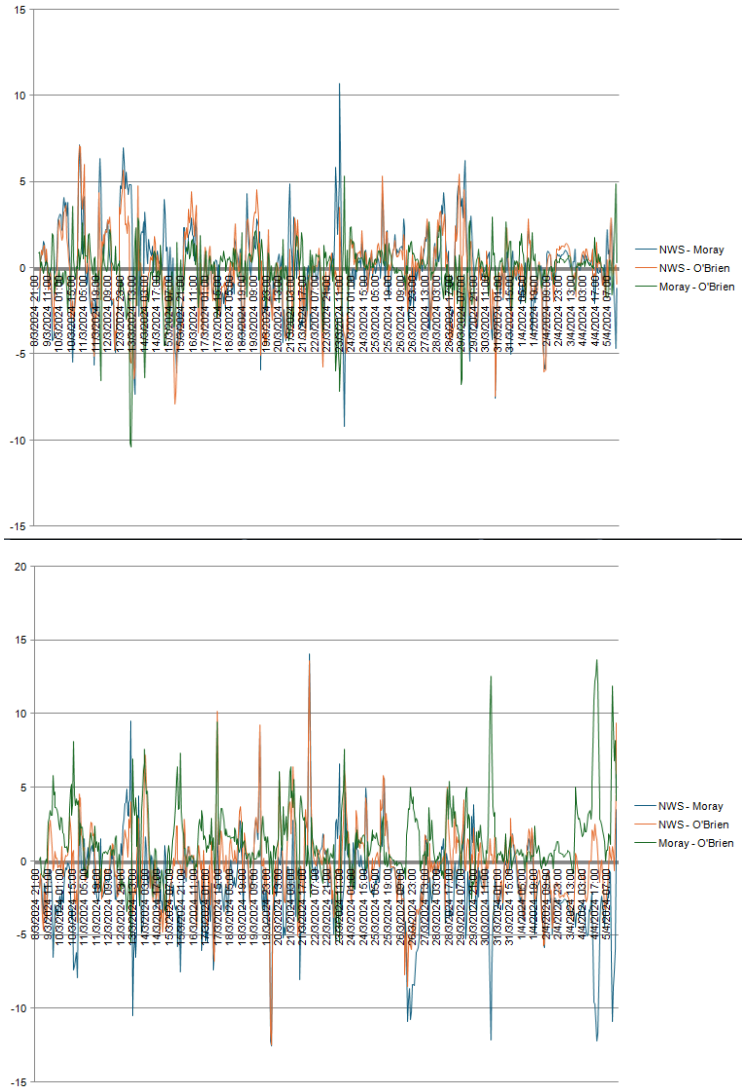

Figure 11. (a) Temperature differences in degrees Fahrenheit between kestrel drop devices at each solar field and the National Weather Service station at Dane County Regional Airport in west Madison (b) Similar, but for dewpoint in degrees Fahrenheit.

Picarro Gas Scouter

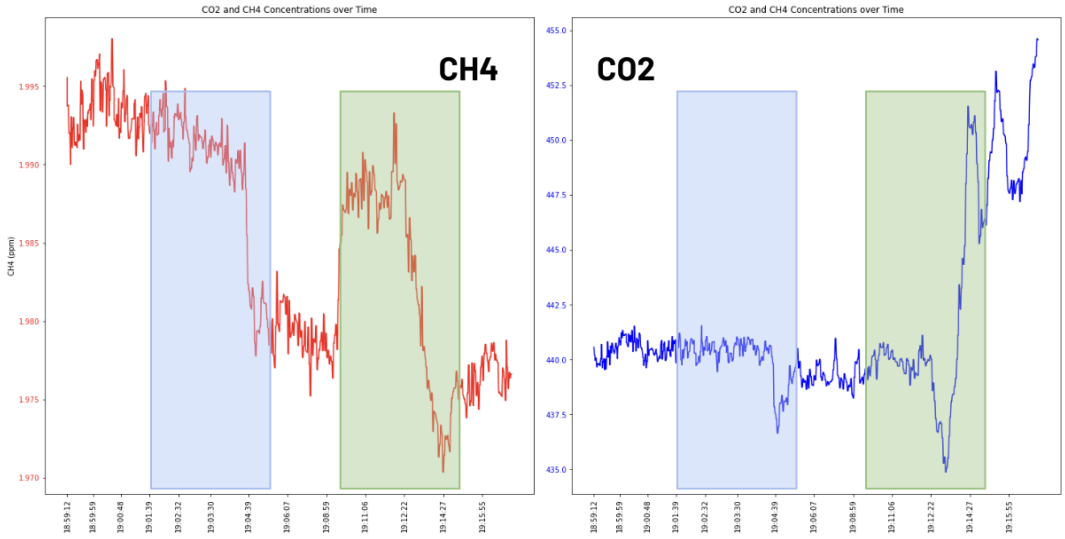

Figure 14. Recorded methane (CH4) and carbon dioxide (CO2) levels overtime at Tripod A location on 5 April 2024. Blue represents measurements under the tripod, green represents measurements under the solar panels.

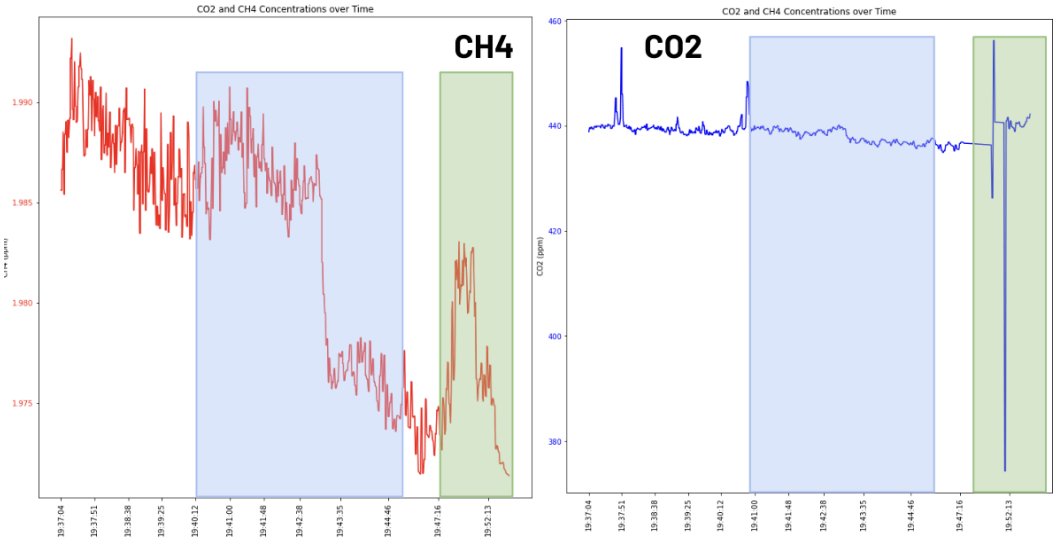

Figure 15. Recorded methane (CH4) and carbon dioxide (CO2) levels overtime at Tripod C location on 5 April 2024. Blue represents measurements under the tripod, green represents measurements under the solar panels.

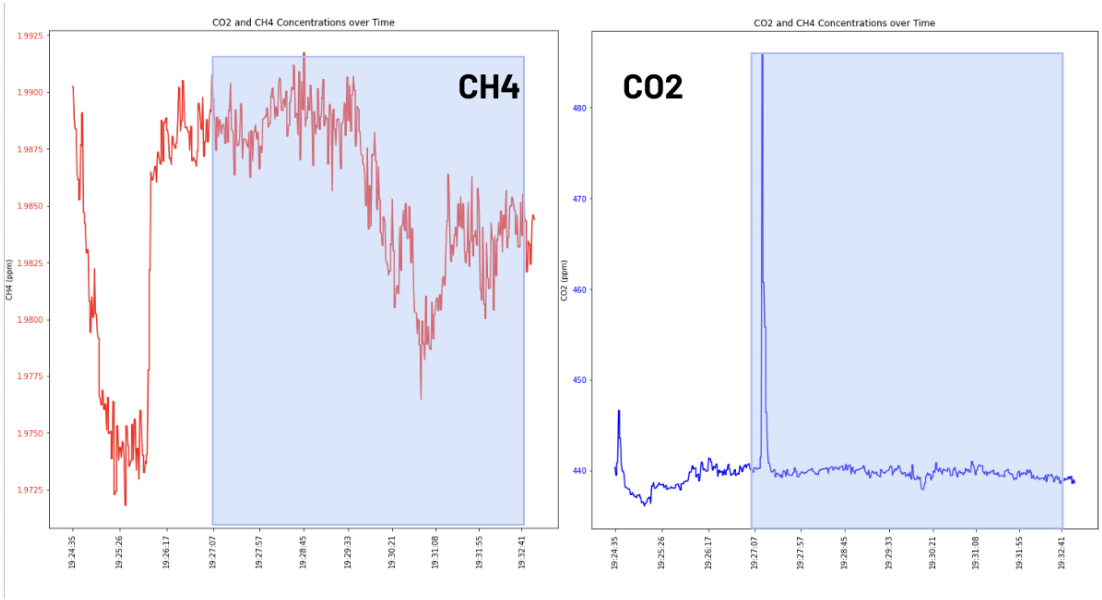

Figure 16. Recorded methane (CH4) and carbon dioxide (CO2) levels overtime at Tripod B location on 5 April 2024. Blue represents measurements under the tripod.

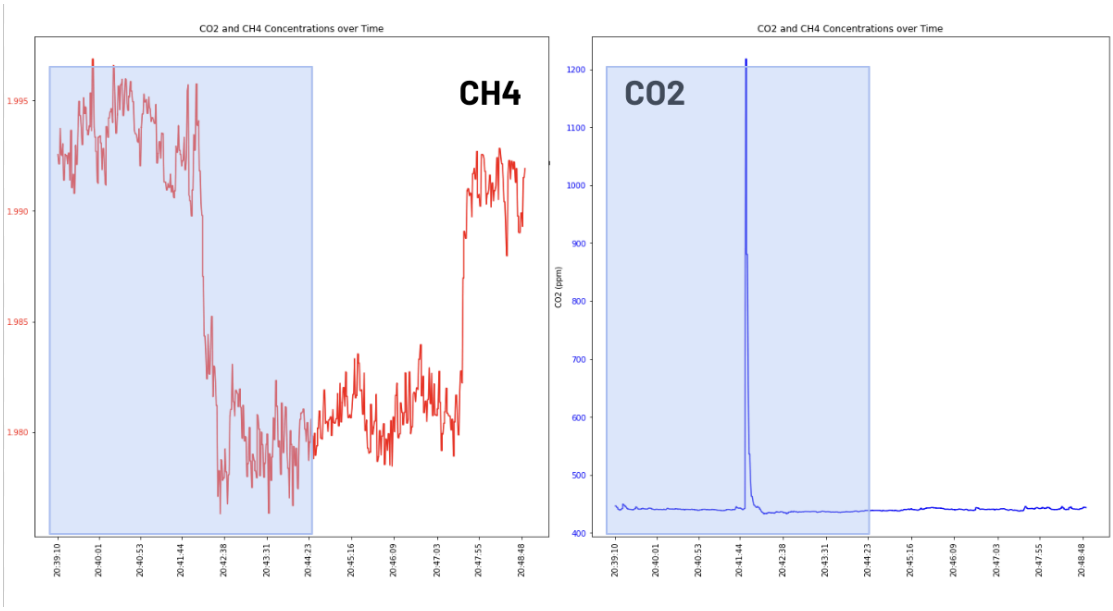

Figure 17. Recorded methane (CH4) and carbon dioxide (CO2) levels overtime at Tripod D location on 5 April 2024. Blue represents measurements under the tripod.

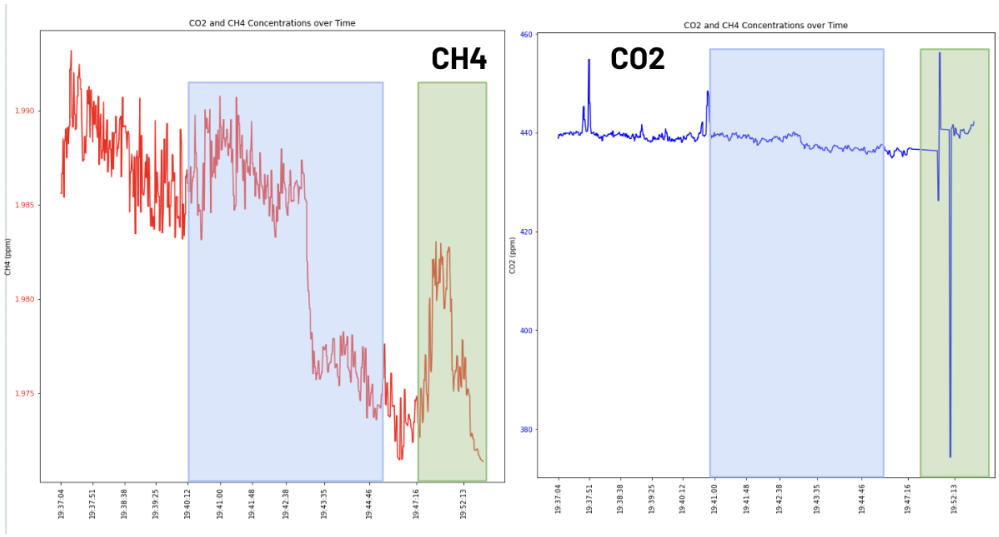

Figure 18. Recorded methane (CH4) and carbon dioxide (CO2) levels overtime at Tripod E location on 5 April 2024. Blue represents measurements under the tripod, green represents measurements under the solar panels.

Tethersonde

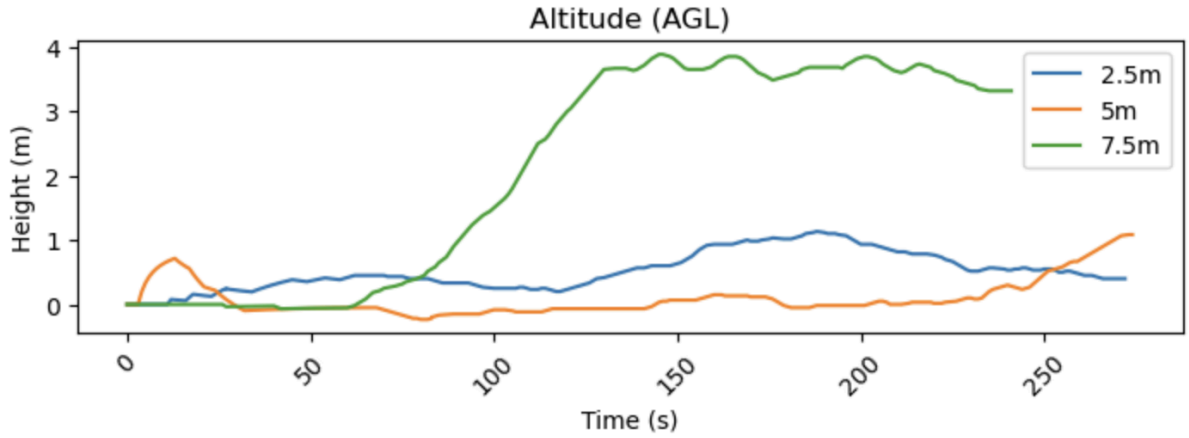

Figure 12. Smoothed time series of altitude above ground level [meters] for the 2.5m, 5m, and 7.5m runs on 5 April 2024.

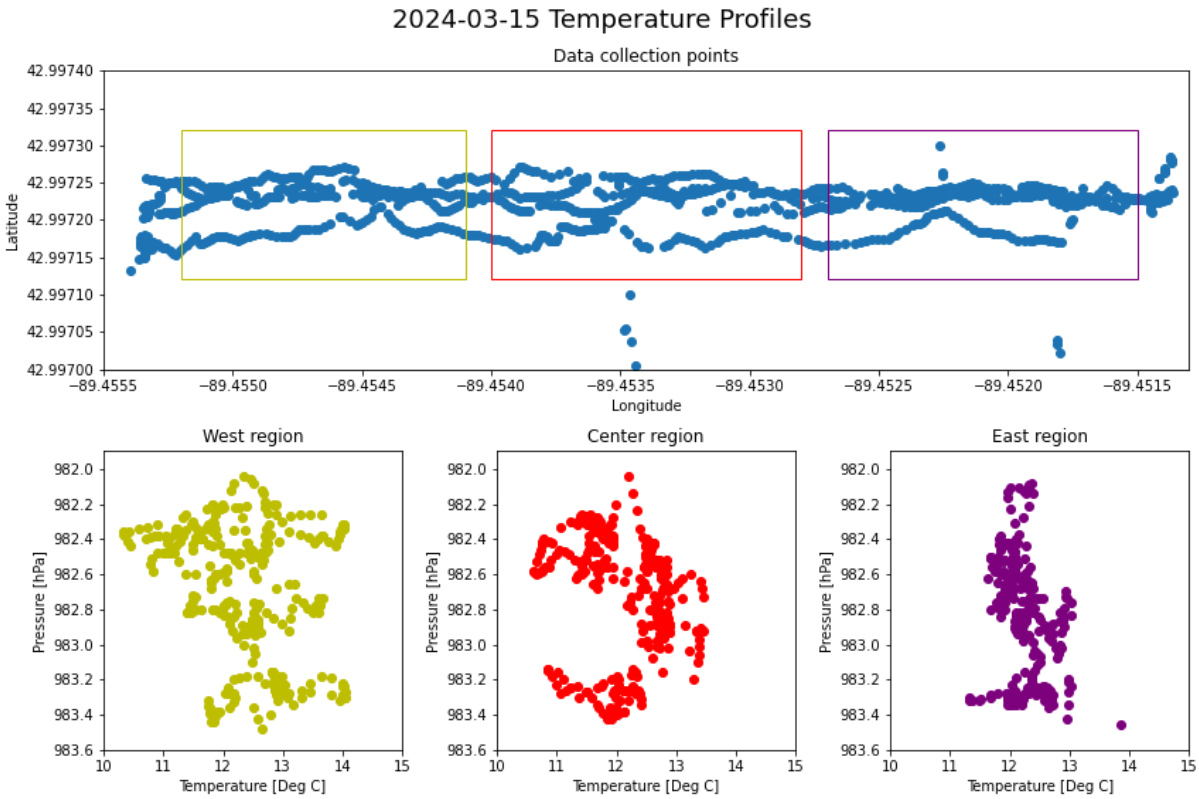

Figure 13. (Top) Latitude and longitude coordinates associated with each data point. Yellow, red, and purple boxes represent data points for the “West”, “Center”, and “East” regions respectively. (Bottom) Profiles of temperature [Deg C] and pressure [hPa] for each region outlined in the top.